Progress In Electromagnetics Research, PIER 22, 85–105, 1999

A NEW FORMULA FOR THE EVALUATION OF THE IMPEDANCE MATRIX IN THE METHOD OF MOMENTS

C. Su

Dept. of Applied Math.
Northwestern Polytechnical University
Xian, Shaanxi, P.R. China

T. K. Sarkar

Dept of Electrical and Computer Engineering
Syracuse University
Syracuse, NY 13244, USA

1. INTRODUCTION

The moment method [1–2] is the most important and well-established numerical technique in computational electromagnetics. The two steps in the moment method are to compute the impedance matrix and to solve the dense matrix equation, which are very time-consuming, particularly for large number of subsections. The major computational difficulty in implementing Galerkin's method is that virtually for all practical cases the inner products need to be evaluated numerically. In particular the task of evaluating the two double integrals (in 2D and a sixfold integrals (in 3D) can be quite difficult and time-consuming for non-smooth kernel functions.

To speed up the moment method, one path is to explore the fast algorithms of solving the dense matrix equation, which include the

wavelet moment method [3–5], the impedance matrix localization (IML) method [Canning 1990, 1993][6–7], the fast multipole method (FMM) (Coifman et al., 1993) [8–9], the matrix decomposition algorithm (MDA) [Michielssen and Boag, 1994][10–12], adaptive multiscale moment method (AMMM) [13–15]. Another path is to find a fast method to compute the impedance matrix, which is the multiple integral involving the Green's function. One possible method is the conjugate gradient-fast Fourier transform method (CG-FFT) [16–19], which does not need to compute and save the impedance matrix. Another method is the adaptive integral method [20]. In the AIM algorithm, the impedance matrix is represented through a sum of near-field and far-field zone components. The near-field component is computed by using the conventional moment method with the Galerkin discretization scheme, utilizing arbitrary local-support basis functions. The far-field components are calculated by using the Galerkin method as well, with a set of auxiliary basis functions which are constructed as superpositions of pointlike current element located on uniformly spaced Cartesian grid nodes. In fact, this method can only obtain an approximate value of the impedance matrix. These two methods cannot deal well with the singular integrals of the impedance matrix elements.

The purpose of this paper is to describe a new formula to compute the impedance matrix. According to the properties of the Green's function, the basis function, and Fourier transform, the hexaple or quadruple integral of the impedance matrix elements in three or two dimension can be simplified to one triple or double integral. For the two common types of basis functions, such as roof-top function and the product of the two triangular functions, the computing formula are presented. The singularity of the integral can easily be removed through a suitable variable transform. The accuracy and efficiency of computing the impedance matrix with this method is much better than other methods. By use of these new formulas, numerical examples of scattering problems of the conducting plates are studied.

2. COMPUTING FORMULA FOR IMPEDANCE MATRIX ELEMENTS

When considering the scattering or radiation problems of electromagnetic fields, we use the moment method. By the use of the Galerkin discretization scheme, that is, choosing the same set of basis functions as the trial and the testing functions $\phi_n(\vec{r})$, we need to compute the

following the impedance matrix elements:

$$\begin{aligned} z_{n,m} &= \int \phi_n(\vec{r}) d^3\vec{r} \int K(\vec{r},\vec{r}\,')\phi_m(\vec{r}\,') d^3\vec{r}\,' \\ \vec{r} &= (x_1, x_2, x_3), \quad \vec{r}\,' = (x_1', x_2', x_3') \end{aligned} \tag{1}$$

$$\begin{aligned} \widetilde{z}_{n,m} &= \int \frac{\partial}{\partial x_i}\phi_n(\vec{r}) d^3\vec{r} \int \frac{\partial}{\partial x_j'}\phi_m(\vec{r}\,') \cdot K(\vec{r},\vec{r}\,') d^3\vec{r}\,' \\ i &= 1,2,3; \quad j = 1,2,3 \end{aligned} \tag{2}$$

where $K(\vec{r},\vec{r}\,')$ is the kernel function.

For one dimensional case, the kernel function $K(\vec{r},\vec{r}\,')$ is the Hankel function $H_0^{(2)}(k\,|x - x'|)$, where k is the wave number in the given medium. The basis functions can be chosen as the sine or cosine functions, triangular basis functions, B-spline basis functions, pulse or hat basis functions.

For two or three dimensional case, the kernel function $K(\vec{r},\vec{r}\,')$ is the Green function $\exp[jk\,|\vec{r} - \vec{r}\,'|]/(4\pi\,|\vec{r} - \vec{r}\,'|)$, where k is the wave number in the given medium. The basis functions always are chosen as the pulse and rooftop basis functions in two dimension. The computation of the impedance matrix is very time-consuming, especially for the large object, because one need to compute hexaple integral for three dimension or quadruple integral for two dimension.

For some cases, we can simplify these integrals into just one triplex integral and one double integral for three dimension and two dimension, respectively. Here we only consider the two dimensional case.

Defining the two-dimensional Fourier transform and inverse transform as

$$\begin{aligned} F\{a(\vec{r})\} &= \iint_{\Omega} a(\vec{r}) \exp[-j\vec{\omega}\cdot\vec{r}] d^2\vec{r} = A(\vec{\omega}) \\ \vec{r} &= (x_1, x_2), \qquad \vec{\omega} = (\omega_1, \omega_2) \\ F^{-1}\{A(\vec{\omega})\} &= \iint_{\Omega} A(\vec{\omega}) \exp[j\vec{\omega}\cdot\vec{r}] d^2\vec{\omega} = a(\vec{r}) \\ \Omega &= (-\infty, \infty) \times (-\infty, \infty) \end{aligned} \tag{3}$$

The following properties of the two-dimensional Fourier transform are needed.

$$a(\vec{r} - \vec{r}_0) \leftrightarrow \exp\left[-j\vec{r}_0\cdot\vec{\omega}\right] A(\vec{\omega}) \tag{4a}$$

$$\frac{\partial a(\vec{r})}{\partial x_i} \leftrightarrow j\omega_i A(\vec{\omega}) \tag{4b}$$

$$a(\vec{r})b(\vec{r}) \leftrightarrow \frac{1}{(2\pi)^2} A(\vec{\omega}) * B(\vec{\omega}) \tag{4c}$$

$$a(\vec{r}) * b(\vec{r}) \leftrightarrow A(\vec{\omega})B(\vec{\omega}) \tag{4d}$$

Suppose the basis function $\alpha_n(\vec{r})$ and the weighting function $\beta_n(\vec{r})$ should satisfy the following equation

$$\phi_n(\vec{r}) = \phi_0(\vec{r} - \vec{r}_n), \qquad \vec{r}_0 = (0,0) \tag{5}$$

$$\Phi_0(\vec{\omega}) = F\left[\phi_0(\vec{r})\right] = \Phi_0(-\vec{\omega}) \tag{6}$$

Then, the Fourier transforms of the basis function, weighting function and Green's function have the following formula

$$\Phi_n(\vec{\omega}) = F\left[\phi_n(\vec{r})\right] = F\left[\phi_0(\vec{r} - \vec{r}_n)\right] = \Phi_0(\vec{\omega}) \exp\left[-j\vec{\omega} \cdot \vec{r}_n\right] \tag{7}$$

$$\hat{G}(\vec{\omega}) = F\left[G(\vec{r})\right] = F\left[\frac{\exp\left[-jk\sqrt{x^2+y^2}\right]}{4\pi\sqrt{x^2+y^2}}\right] = \hat{G}(-\vec{\omega}) \tag{8}$$

From the above formulas (4)–(8), we can derive

$$\begin{aligned}
&\int_\Omega \alpha_n(\vec{r}) d^2\vec{r} \int_\Omega \beta_m(\vec{r}\,') G(\vec{r} - \vec{r}\,') d^2\vec{r}\,' \\
&\quad = \int_\Omega \alpha_n(\vec{r}) G(\vec{r}) * \beta_m(\vec{r}) d^2\vec{r} \\
&\quad = F\left[\alpha_n(\vec{r}) G(\vec{r}) * \beta_m(\vec{r})\right] \Big|_{\vec{\omega}=0} \\
&\quad = (2\pi)^{-2} F\left[\alpha_n(\vec{r})\right] * F\left[G(\vec{r}) * \beta_m(\vec{r})\right] \Big|_{\vec{\omega}=0} \\
&\quad = (2\pi)^{-2} F\left[\alpha_n(\vec{r})\right] * \left[F\left[G(\vec{r})\right] \cdot F\left[\beta_m(\vec{r})\right]\right] \Big|_{\vec{\omega}=0} \\
&\quad = (2\pi)^{-2} \left[A_n(\vec{\omega})\right] * \left[\hat{G}(\vec{\omega}) B_m(\vec{\omega})\right] \Big|_{\vec{\omega}=0} \\
&\quad = (2\pi)^{-2} \int_\Omega A_n(\vec{\theta}) \hat{G}(\vec{\omega} - \vec{\theta}) B_m(\vec{\omega} - \vec{\theta}) d^2\vec{\theta} \Big|_{\vec{\omega}=0} \\
&\quad = (2\pi)^{-2} \int_\Omega A_n(\vec{\theta}) \hat{G}(-\vec{\theta}) B_m(-\vec{\theta}) d^2\vec{\theta} \\
&\quad = (2\pi)^{-2} \int_\Omega A_0(\vec{\theta}) \exp\left[-j\vec{\theta} \cdot \vec{r}_n\right] \hat{G}(-\vec{\theta}) B_0(-\vec{\theta}) \exp\left[+j\vec{\theta} \cdot \vec{r}_m\right] d^2\vec{\theta}
\end{aligned}$$

$$
\begin{aligned}
&= (2\pi)^{-2} \int_{\Omega} A_0(\vec{\theta}) \hat{G}(-\vec{\theta}) B_0(-\vec{\theta}) \exp\left[+j\vec{\theta}\cdot(\vec{r}_m - \vec{r}_n)\right] d^2\vec{\theta} \\
&= F^{-1}\left[A_0(\vec{\theta})\hat{G}(-\vec{\theta})B_0(-\vec{\theta})\right]\Big|_{\vec{r}=\vec{r}_m-\vec{r}_n} \\
&= F^{-1}\left[A_0(\vec{\theta})B_0(\vec{\theta})\hat{G}(\vec{\theta})\right]\Big|_{\vec{r}=\vec{r}_m-\vec{r}_n} \\
&= F^{-1}\left[A_0(\vec{\theta})B_0(\vec{\theta})\right] * F^{-1}\left[\hat{G}(\vec{\omega})\right]\Big|_{\vec{r}=\vec{r}_m-\vec{r}_n} \\
&= G(\vec{r}) * \psi(\vec{r})\Big|_{\vec{r}=\vec{r}_m-\vec{r}_n} \\
&= \int_{\Omega} G(\vec{r}_m - \vec{r}_n - \vec{r})\psi(\vec{r}) d^2\vec{r} = \int_{\Omega} G(\vec{r} + \vec{r}_n - \vec{r}_m)\psi(\vec{r}) d^2\vec{r}
\end{aligned} \tag{9}
$$

$$
\begin{aligned}
&\int_{\Omega} \frac{\partial \alpha_n(\vec{r})}{\partial x_i} d^2\vec{r} \int_{\Omega} \frac{\partial \beta_m(\vec{r}\,')}{\alpha x'_j} G(\vec{r} - \vec{r}\,') d^2\vec{r}\,' \\
&\quad = (2\pi)^{-2} F\left[\frac{\partial \alpha_n(\vec{r})}{\partial x_i}\right] * \left[F\left[G(\vec{r})\right] \cdot F\left[\frac{\partial \beta_m(\vec{r})}{\partial x_j}\right]\right]\Big|_{\vec{\omega}=0} \\
&\quad = (2\pi)^{-2}\left[j\omega_i A_n(\vec{\omega})\right] * \left[j\omega_j\left[\hat{G}(\vec{\omega})B_m(\vec{\omega})\right]\right]\Big|_{\vec{\omega}=0} \\
&\quad = -(2\pi)^{-2} \int_{\Omega} \theta_i A_n(\vec{\theta})(\omega_j - \theta_j)\hat{G}(\vec{\omega} - \vec{\theta}) B_m(\vec{\omega} - \vec{\theta}) d^2\vec{\theta}\Big|_{\vec{\omega}=0} \\
&\quad = (2\pi)^{-2} \int_{\Omega} \theta_i\theta_j A_n(\vec{\theta})\hat{G}(-\vec{\theta}) B_m(-\vec{\theta}) d^2\vec{\theta} \\
&\quad = F^{-1}\left[\theta_i\theta_j A_0(\vec{\theta})B_0(-\vec{\theta})\hat{G}(\vec{\theta})\right]\Big|_{\vec{r}=\vec{r}_m-\vec{r}_n} \\
&\quad = F^{-1}\left[\theta_i\theta_j A_0(\vec{\theta})B_0(\vec{\theta})\right] * F^{-1}\left[\hat{G}(\vec{\omega})\right]\Big|_{\vec{r}=\vec{r}_m-\vec{r}_n} \\
&\quad = -G(\vec{r}) * \left[\frac{\partial \alpha_0(\vec{r})}{\partial x_i} * \frac{\partial \beta_0(\vec{r})}{\partial x_j}\right]\Big|_{\vec{r}=\vec{r}_m-\vec{r}_n} \\
&\quad = -\int_{\Omega} G(\vec{r} + \vec{r}_n - \vec{r}_m)\Psi_{i,j}(\vec{r}) d^2\vec{r}
\end{aligned} \tag{10}
$$

where $\psi(\vec{r}) = \alpha_0(\vec{r}) * \beta_0(\vec{r})$, $\Psi_{i,j}(\vec{r}) = \frac{\partial \alpha_0(\vec{r})}{\alpha x_i} * \frac{\partial \beta_0(\vec{r})}{\partial x_j}$.

From the formula (9) and (10), if the basis function and weighting function are of a finite support, the original quadruple integral can be simplified to one double integral in that region.

The formula (9) and (10) are also valid for the three dimensional case. The only difference is that the double integral become the one triple integral.

Now, we discuss the computing formula for specific basis and weighting functions.

(A) For the basis function and the weighting function constructed by product of the two triangular functions. Suppose

$$\alpha_0(\vec{r}) = \beta_0(\vec{r}) = \phi(\vec{r}) = \phi_0(x)\phi_0(y),$$
$$\phi_0(x) = \begin{cases} \left(1 - \dfrac{|x|}{T}\right) & |x| \le T \\ 0 & \text{other} \end{cases},$$

then

$$\Phi(\vec{\omega}) = F\left[\phi(\vec{r})\right] = T^2 \sin c^2\left[\omega_x T/2\right] \sin c^2\left[\omega_y T/2\right] = \Phi(-\vec{\omega})$$
$$f(x) \equiv \phi_0'(x) * \phi_0'(x) = \frac{1}{T}\begin{cases} 2 - |x/T| & T \le |x| \le 2T \\ -2 + 3\,|x/T| & 0 \le |x| \le T \\ 0 & \text{other} \end{cases}$$
$$F(x) \equiv \phi_0(x) * \phi_0(x) = \begin{cases} \dfrac{(2T+x)^3}{6T^2} & [-2T, -T] \\ \dfrac{2T}{3} - \dfrac{x^2}{T} - \dfrac{x^3}{2T^2} & [-T, 0] \\ \dfrac{2T}{3} - \dfrac{x^2}{T} - \dfrac{x^3}{2T^2} & [0, T] \\ \dfrac{(2T-x)^3}{6T^2} & [T, 2T] \\ 0 & |x| \ge 2T \end{cases}$$
$$H(x) \equiv \phi_0(x) * \phi_0'(x) = \begin{cases} \dfrac{(2 + x/T)^2}{2} & [-2T, -T] \\ -2\dfrac{x}{T} - \dfrac{3x^2}{2T^2} & [-T, 0] \\ -2\dfrac{x}{T} + \dfrac{3x^2}{2T^2} & [0, T] \\ -\dfrac{(-2 + x/T)^2}{2} & [T, 2T] \\ 0 & |x| \ge 2T \end{cases}$$

$$\int_\Omega \alpha_n(\vec{r})d\vec{r} \int_\Omega \beta_m(\vec{r}\,')G(\vec{r} - \vec{r}\,')d\vec{r}\,'$$
$$= \int_D G(\vec{r} + (\vec{r}_n - \vec{r}_m))F(x)F(y)d\vec{r} \equiv A(\vec{r}_n - \vec{r}_m)$$

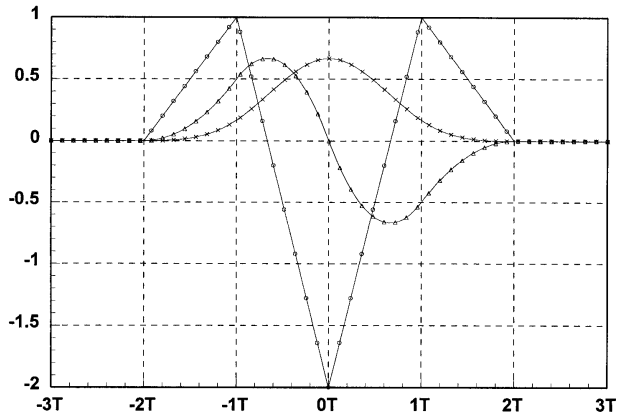

Figure 1. The curve of $\frac{1}{T}\phi_0(x) * \phi_0(x)$ $(\times)$, $\phi_0(x) * \phi_0'(x)$ $(\triangle)$, $T\phi_0'(x) * \phi_0'(x)$ $(\circ)$.

$$\int_\Omega \frac{\partial}{\partial x}\alpha_n(\vec{r})d\vec{r}\int_\Omega \frac{\partial}{\partial x'}\beta_m(\vec{r}\,')G(\vec{r}-\vec{r}\,')d\vec{r}\,'$$
$$= -\int_D G(\vec{r}+(\vec{r}_n-\vec{r}_m))f(x)F(y)d\vec{r} \equiv -A_{xx}(\vec{r}_n-\vec{r}_m)$$
$$\int_\Omega \frac{\partial}{\partial y}\alpha_n(\vec{r})d\vec{r}\int_\Omega \frac{\partial}{\partial y'}\beta_m(\vec{r}\,')G(\vec{r}-\vec{r}\,')d\vec{r}\,'$$
$$= -\int_D G(\vec{r}+(\vec{r}_n-\vec{r}_m))F(x)f(y)d\vec{r} \equiv -A_{yy}(\vec{r}_n-\vec{r}_m)$$
$$\int_\Omega \frac{\partial}{\partial y}\alpha_n(\vec{r})d\vec{r}\int_\Omega \frac{\partial}{\partial x'}\beta_m(\vec{r}\,')G(\vec{r}-\vec{r}\,')d\vec{r}\,'$$
$$= -\int_D G(\vec{r}+(\vec{r}_n-\vec{r}_m))H(x)H(y)d\vec{r} \equiv -A_{yx}(\vec{r}_n-\vec{r}_m)$$
$$\int_\Omega \frac{\partial}{\partial x}\alpha_n(\vec{r})d\vec{r}\int_\Omega \frac{\partial}{\partial y'}\beta_m(\vec{r}\,')G(\vec{r}-\vec{r}\,')d\vec{r}\,'$$
$$= -\int_D G(\vec{r}+(\vec{r}_n-\vec{r}_m))H(y)H(x)d\vec{r} \equiv -A_{xy}(\vec{r}_n-\vec{r}_m)$$

where $D=\{(x,y);\ |x|\le 2T,\ |y|\le 2T\}$.

The curves of $F(x)$, $f(x)$, $H(x)$ are plotted in following figure (Fig. 1).

If $\vec{r}_n=(iT,jT)$, then $A(\vec{r})$, $A_{xx}(\vec{r})$, $A_{yy}(\vec{r})$, $A_{yx}(\vec{r})$, $A_{xy}(\vec{r})$ have the following representation:

(1) $A_{xx}(x,y)=A_{yy}(y,x)$, $A_{yx}(x,y)=A_{xy}(y,x)$

(2) $A(iT, jT) = A(\pm iT, \pm jT),\ A_{xx}(iT, jT) = A_{xx}(\pm iT, \pm jT)$
$A_{xy}(iT, jT) = A_{xy}(-iT, -jT) = -A_{xy}(-iT, jT) = -A_{xy}(iT, -jT)$

When $\vec{r}_n = (iT, jT)(i, j = 0, \pm 1, \pm 2)$ is in the region D, the singular point of Green's function in the integrals can be removed easily through a suitable variable transform. For example, $A(0, 0)$ can be determined by

$$A(0,0) = \frac{1}{\pi}\left[\int_0^{\pi/4} d\theta \int_0^{2T/\cos\theta} \exp[-jkr]F(r\cos\theta)F(r\sin\theta)dr + \int_{\pi/4}^{\pi/2} d\theta \int_0^{2T/\cos\theta} \exp[-jkr]F(r\cos\theta)F(r\sin\theta)dr\right]$$

The real and imaginary part of $A(x, y),\ A_{xx}(y, x),\ A_{xy}(x, y)$ with $T = 0.061$ are plotted in Figure 2, 3, 4.

For the three dimensional case, $A(\vec{r}_n),\ A_{xx}(\vec{r}_n)$ and $A_{xy}(\vec{r}_n)$, can be computed by

$$A(\vec{r}_n) = \int_{D^3} G(\vec{r} + \vec{r}_n)F(x)F(y)F(z)d\vec{r}$$
$$A_{xx}(\vec{r}_n) = \int_{D^3} G(\vec{r} + \vec{r}_n)f(x)F(y)F(z)d\vec{r}$$
$$A_{xy}(\vec{r}_n) = \int_{D^3} G(\vec{r} + \vec{r}_n)H(x)H(y)F(z)d\vec{r}$$

where $D^3 = \{(x, y, z);\ |x| \le 2T,\ |y| \le 2T,\ |z| \le 2T\}$.

(B) for the roof-top basis function

If

$$\alpha_0(\vec{r}) = \phi_0(x)\psi_0(y), \quad \beta_0(\vec{r}) = \phi_0(y)\psi_0(x),$$
$$\phi_0(t) = \begin{cases} \left(1 - \dfrac{|t|}{T}\right) & |t| \le T \\ 0 & \text{other} \end{cases}, \quad \psi_0(t) = \begin{cases} 1 & |t| \le T/2 \\ 0 & \text{other} \end{cases}$$

then

$$A_0(\vec{\omega}) = F\left[\alpha_0(\vec{r})\right] = T^2 \sin c^2\left[\omega_x T/2\right] \sin c\left[\omega_y T/2\right] = A_0(-\vec{\omega})$$
$$B_0(\vec{\omega}) = F\left[\beta_0(\vec{r})\right] = T^2 \sin c\left[\omega_x T/2\right] \sin c^2\left[\omega_y T/2\right] = B_0(-\vec{\omega})$$

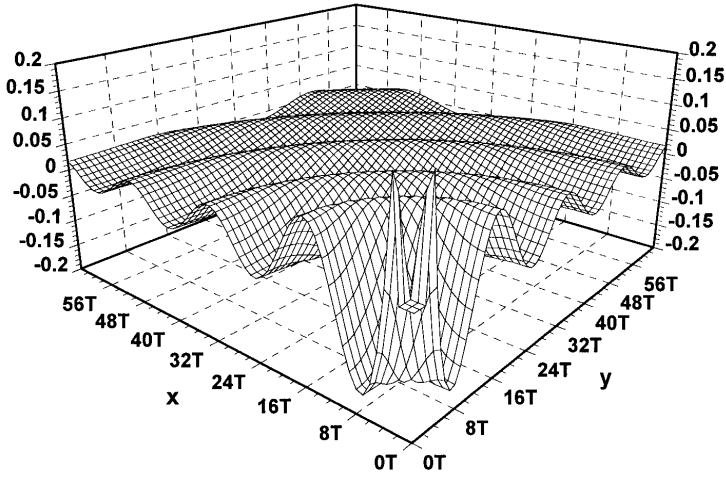

(a) real part of $A(x,y)\cdot T^{-4}$, $A(0,0)T^{-4}=2.68$, $A(0,1)T^{-4}=A(1,0)T^{-4}=1.43$, $A(0,2)T^{-4}=A(2,0)T^{-4}=0.50$, $A(1,1)T^{-4}=0.91$, $A(2,1)T^{-4}=A(1,2)T^{-4}=0.40$, $A(2,2)T^{-4}=0.23$.

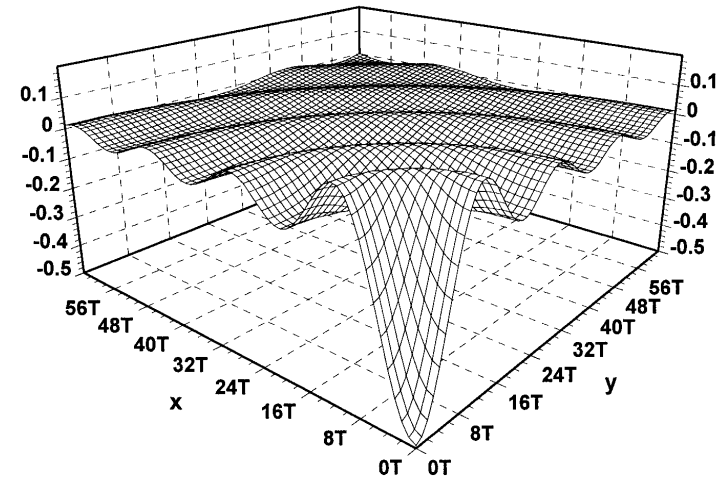

(b) imaginary part of $A(x,y)\cdot T^{-4}$.

Figure 2. The real and imaginary part of $A(x,y)$.

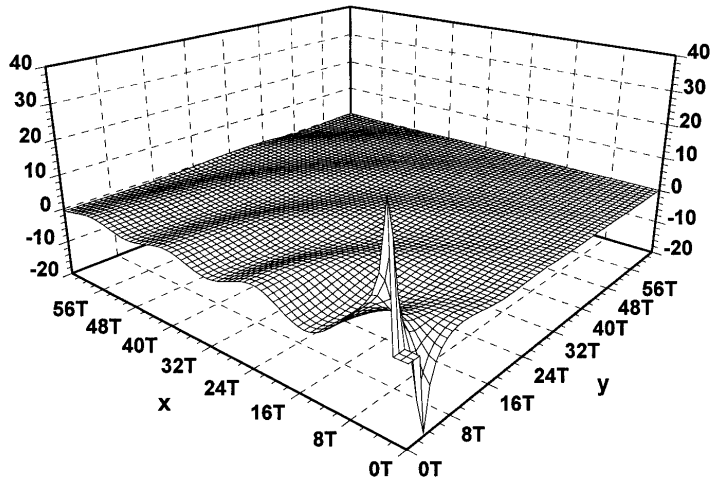

(a) real part of $A_{xx}(x,y)\cdot T^{-4}$, $A_{xx}(0,0)T^{-4}=-1044.96$, $A_{xx}(0,1)\cdot T^{-4}=-404.23$, $A_{xx}(1,0)T^{-4}=-314.80$, $A_{xx}(0,1)T^{-4}=74.41$, $A_{xx}(0,2)T^{-4}=-59.53$, $A_{xx}(2,0)T^{-4}=129.94$, $A_{xx}(1,2)T^{-4}=-19.89$, $A_{xx}(2,1)T^{-4}=64.25$, $A_{xx}(2,2)T^{-4}=8.75$.

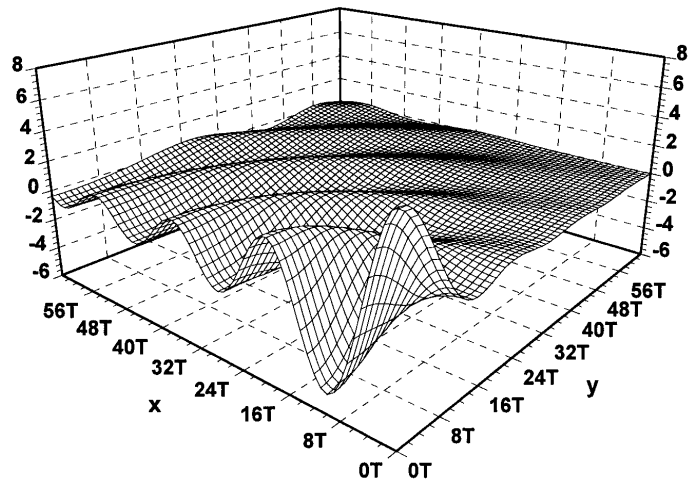

(b) imaginary part of $A_{xx}(x,y)\cdot T^{-4}$.

Figure 3. The real and imaginary part of $A_{xx}(x,y)$.

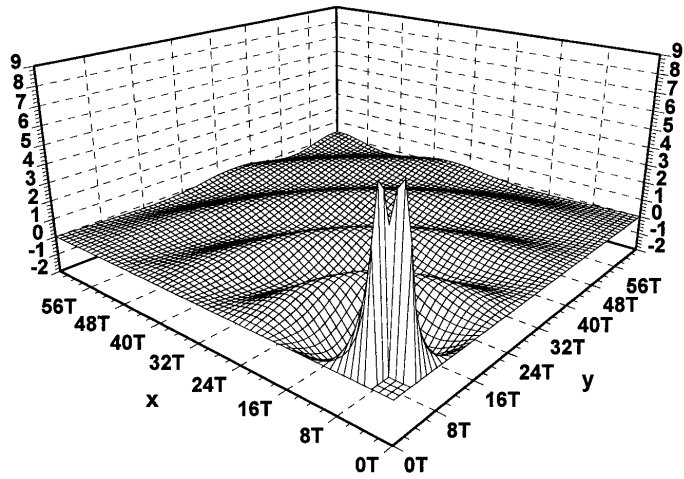

(a) real part of $A_{xy}(x,y)\cdot T^{-4}$, $A_{xy}(0,0)=A_{xy}(1,0)=A_{xy}(0,1)=A_{xy}(2,0)=A_{xy}(0,2)=0$, $A_{xy}(1,1)T^{-4}=277.76$, $A_{xy}(2,1)T^{-4}=A_{xy}(1,2)T^{-4}=51.69$, $A_{xy}(2,2)T^{-4}=31.96$, $A_{xy}(3,1)T^{-4}=A_{xy}(1,3)T^{-4}=13.81$, $A_{xy}(3,2)T^{-4}=A_{xy}(2,3)T^{-4}=15.34$, $A_{xy}(3,3)T^{-4}=11.34$.

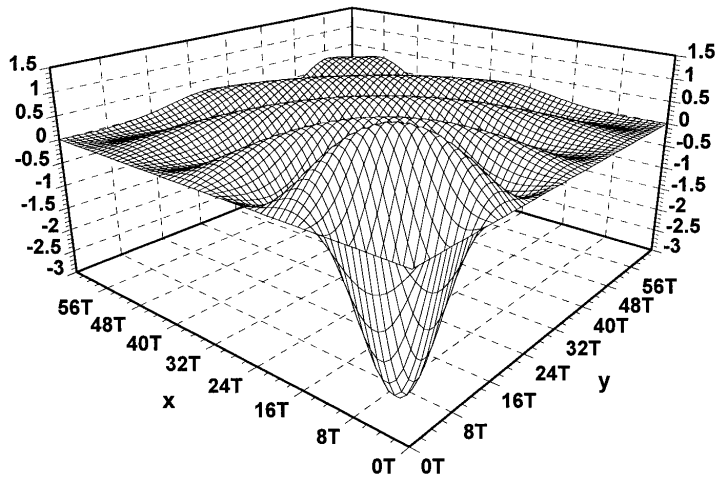

(b) imaginary part of $A_{xy}(x,y)\cdot T^{-4}$.

Figure 4. The real and imaginary part of $A_{xy}(x,y)$.

$$F(x) \equiv \phi_0(x) * \phi_0(x) = \begin{cases} \dfrac{(2T+x)^3}{6T^2} & [-2T, -T] \\ \dfrac{2T}{3} - \dfrac{x^2}{T} - \dfrac{x^3}{2T^2} & [-T, 0] \\ \dfrac{2T}{3} - \dfrac{x^2}{T} + \dfrac{x^3}{2T^2} & [0, T] \\ \dfrac{(2T-x)^3}{6T^2} & [T, 2T] \\ 0 & |x| \geq 2T \end{cases}$$

$$f(x) \equiv \phi_0'(x) * \phi_0'(x) = \frac{1}{T} \begin{cases} -2 + |x/T| & T \leq |x| \leq 2T \\ 2 - 3\,|x/T| & 0 \leq |x| \leq T \\ 0 & \text{other} \end{cases}$$

$$g(x) \equiv \psi_0(x) * \psi_0(x) = \begin{cases} T + x & -T \leq x \leq 0 \\ T - x & 0 \leq x \leq T \\ 0 & \text{other} \end{cases}$$

$$H(x) \equiv \phi_0'(x) * \psi_0(x) = \begin{cases} \dfrac{3}{2} + \dfrac{x}{T} & \left[-\dfrac{3}{2}T, -\dfrac{1}{2}T\right] \\ -2\dfrac{x}{T} & \left[-\dfrac{1}{2}T, \dfrac{1}{2}T\right] \\ -\dfrac{3}{2} + \dfrac{x}{T} & \left[\dfrac{1}{2}T, \dfrac{3}{2}T\right] \\ 0 & \text{other} \end{cases}$$

$$\int_\Omega \alpha_n(\vec{r})d\vec{r} \int_\Omega \alpha_m(\vec{r}\,')G(\vec{r} - \vec{r}\,')d\vec{r}\,'$$
$$= \int_C G(\vec{r} + (\vec{r}_n^{\,x} - \vec{r}_m^{\,x}))F(x)g(y)d\vec{r} = A^\alpha(\vec{r}_n^{\,x} - \vec{r}_m^{\,x})$$
$$\int_\Omega \frac{\partial}{\partial x}\alpha_n(\vec{r})d\vec{r} \int_\Omega \frac{\partial}{\partial x'}\alpha_m(\vec{r}\,')G(\vec{r} - \vec{r}\,')d\vec{r}\,'$$
$$= -\int_C G(\vec{r} + (\vec{r}_n^{\,x} - \vec{r}_m^{\,x}))f(x)g(y)d\vec{r} = A_{xx}^\alpha(\vec{r}_n^{\,x} - \vec{r}_m^{\,x})$$
$$\int_\Omega \beta_n(\vec{r})d\vec{r} \int_\Omega \beta_m(\vec{r}\,')G(\vec{r} - \vec{r}\,')d\vec{r}\,'$$
$$= \int_D G(\vec{r} + (\vec{r}_n^{\,y} - \vec{r}_m^{\,y}))F(y)g(x)d\vec{r} = A^\beta(\vec{r}_n^{\,y} - \vec{r}_m^{\,y})$$
$$\int_\Omega \frac{\partial}{\partial y}\beta_n(\vec{r})d\vec{r} \int_\Omega \frac{\partial}{\partial y'}\beta_m(\vec{r}\,')G(\vec{r} - \vec{r}\,')d\vec{r}\,'$$
$$= -\int_D G(\vec{r} + (\vec{r}_n^{\,y} - \vec{r}_m^{\,y}))g(x)f(y)d\vec{r} = A_{yy}^\beta(\vec{r}_n^{\,y} - \vec{r}_m^{\,y})$$

$$\int_\Omega \frac{\partial}{\partial x}\alpha_n(\vec{r})d\vec{r}\int_\Omega \frac{\partial}{\partial y'}\beta_m(\vec{r}\,')G(\vec{r}-\vec{r}\,')d\vec{r}\,'$$
$$= -\int_E G(\vec{r}+(\vec{r}_n^{\,x}-\vec{r}_m^{\,y}))H(x)H(y)d\vec{r} = A_{xy}(\vec{r}_n^{\,x}-\vec{r}_m^{\,y})$$
$$\int_\Omega \frac{\partial}{\partial y}\beta_n(\vec{r})d\vec{r}\int_\Omega \frac{\partial}{\partial x'}\alpha_m(\vec{r}\,')G(\vec{r}-\vec{r}\,')d\vec{r}\,'$$
$$= -\int_E G(\vec{r}+(\vec{r}_n^{\,y}-\vec{r}_m^{\,x}))H(y)H(x)d\vec{r} = A_{yx}(\vec{r}_n^{\,y}-\vec{r}_m^{\,x})$$

where

$$C = \{(x,y); \quad |x| \le 2T, \quad |y| \le T\},$$
$$D = \{(x,y); \quad |x| \le T, \quad |y| \le 2T\},$$
$$E = \{(x,y); \quad |x| \le \frac{3}{2}T, \quad |y| \le \frac{3}{2}T\}.$$

If

$$\vec{r}_n^{\,x} = (iT, jT), \quad \vec{r}_n^{\,y} = ((i+\frac{1}{2})T, \quad (j+\frac{1}{2})T),$$

then $A^\alpha(\vec{r})$, $A^\beta(\vec{r}), A^\alpha_{xx}(\vec{r})$, $A^\beta_{yy}(\vec{r})$, $A_{yx}(\vec{r})$, $A_{xy}(\vec{r})$ have the following formula:

(1) $A^\alpha(x,y) = A^\beta(y,x)$, $A^\alpha_{xx}(x,y) = A^\beta_{yy}(y,x)$, $A_{yx}(x,y) = A_{xy}(y,x)$

(2) $A^\alpha(iT,jT) = A^\alpha(\pm iT, \pm jT)$, $A^\alpha_{xx}(iT,jT) = A^\alpha_{xx}(\pm iT, \pm jT)$, $A_{xy}((i+\frac{1}{2})T,\ (j+\frac{1}{2})T) = A_{xy}(-(i+\frac{1}{2})T,\ -(j+\frac{1}{2})T) = -A_{xy}(-(i+\frac{1}{2})T,\ (j+\frac{1}{2})T) = -A_{xy}((i+\frac{1}{2})T,\ -(j+\frac{1}{2})T)$

The real and imaginary part of $A^\alpha(x,y)$, $A^\alpha_{xx}(y,x)$, $A_{xy}(x,y)$ with $T = 0.061$ are plotted in Figures 5, 6, 7.

For the three dimensional case, $A^\alpha(\vec{r}_n)$, $A^\alpha_{xx}(\vec{r}_n)$ and $A_{xy}(\vec{r}_n)$ can be computed by

$$A^\alpha(\vec{r}_n) = \int_{D^3} G(\vec{r}+\vec{r}_n)F(x)g(y)g(z)d\vec{r}$$
$$A^\alpha_{xx}(\vec{r}_n) = \int_{D^3} G(\vec{r}+\vec{r}_n)f(x)g(y)g(z)d\vec{r}$$
$$A_{xy}(\vec{r}_n) = \int_{E^3} G(\vec{r}+\vec{r}_n)H(x)H(y)g(z)d\vec{r}$$

where

$$D^3 = \{(x,y,z); \quad |x| \le 2T, \quad |y| \le T, \quad |z| \le T\},$$
$$E^3 = \{(x,y,z); \quad |x| \le \frac{3}{2}T, \quad |y| \le \frac{3}{2}T, \quad |z| \le T\}.$$

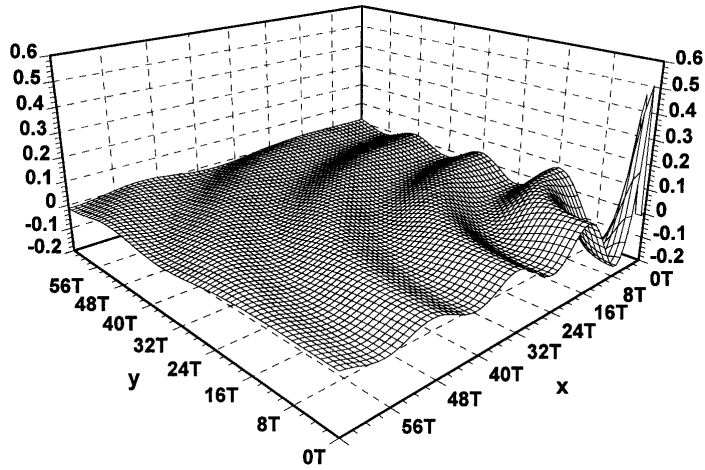

(a) real part of $A^\alpha(x,y)\cdot T^{-4}$, $A^\alpha(0,0)T^{-4}=3.18$, $A^\alpha(0,1)T^{-4}=1.24$, $A^\alpha(1,0)T^{-4}=1.61$, $A^\alpha(1,1)T^{-4}=0.86$, $A^\alpha(0,2)T^{-4}=0.47$, $A^\alpha(1,2)T^{-4}=0.38$, $A^\alpha(2,0)T^{-4}=0.52$, $A^\alpha(2,1)T^{-4}=0.41$, $A^\alpha(2,2)T^{-4}=0.22$.

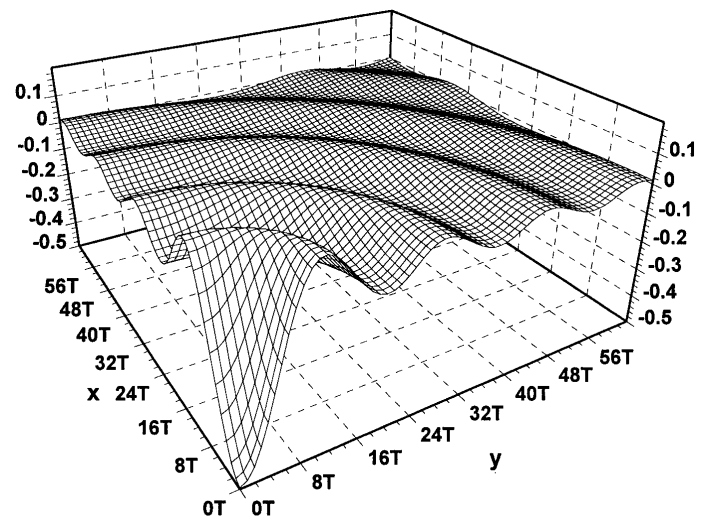

(b) imaginary part of $A^\alpha(x,y)/T^4$.

Figure 5. The real and imaginary part of $A^\alpha(x,y)$.

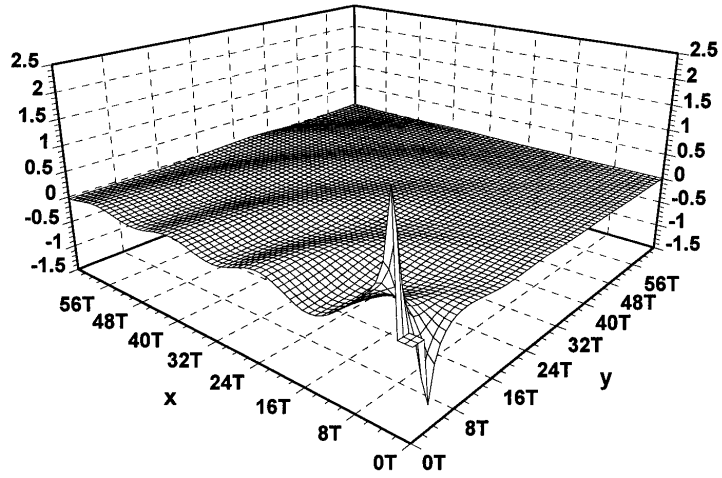

(a) real part of $A^{\alpha}_{xx}(x,y)\cdot T^{-3}$, $A^{\alpha}_{xx}(0,0)T^{-3} = -81.32$, $A^{\alpha}_{xx}(0,1)T^{-3} = -16.66$, $A^{\alpha}_{xx}(1,0)T^{-3} = 26.45$, $A^{\alpha}_{xx}(1,1)T^{-3} = 0.96$, $A^{\alpha}_{xx}(0,2)T^{-3} = -2.97$, $A^{\alpha}_{xx}(1,2)T^{-3} = -1.31$, $A^{\alpha}_{xx}(2,0)T^{-3} = 9.30$, $A^{\alpha}_{xx}(2,1)T^{-3} = 3.40$, $A^{\alpha}_{xx}(2,2)T^{-3} = 0.34$.

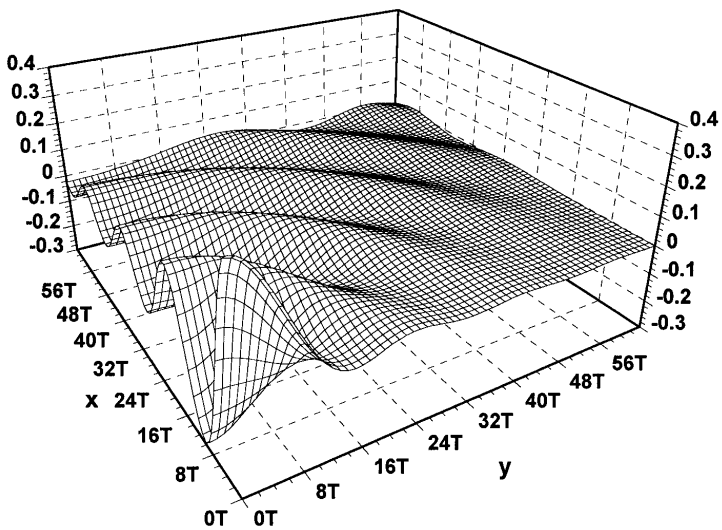

(b) imaginary part of $A^{\alpha}_{xx}(x,y)\cdot T^{-3}$.

Figure 6. The real and imaginary part of $A^{\alpha}_{xx}(x,y)$.

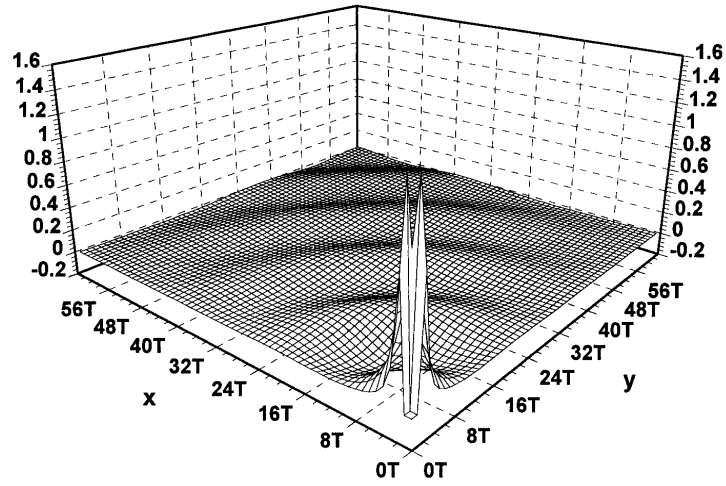

(a) real part of $A_{xy}(x,y)\cdot T^{-3}$, $A_{xy}(\frac{1}{2},\frac{1}{2})T^{-3} = 32.33$, $A_{xy}(\frac{3}{2},\frac{1}{2})T^{-3} = A_{xy}(\frac{1}{2},\frac{3}{2})T^{-3} = 6.85$, $A_{xy}(\frac{3}{2},\frac{3}{2})T^{-3} = 4.56$.

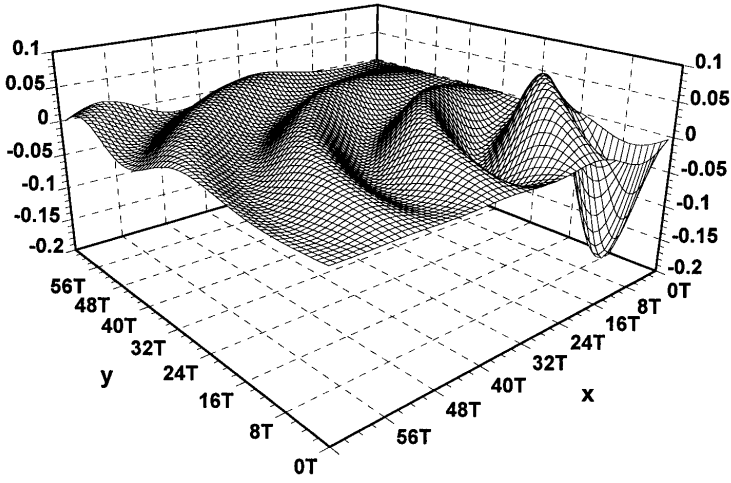

(b) imaginary part of $A_{xy}(x,y)\cdot T^{-3}$.

Figure 7. The real and imaginary part of $A_{xy}(x,y)$.

Although the above formulas are obtained through a uniform subdivision, one can obtain the similar formulas in a straightforward fashion through a non-uniform subdivision.

3. NUMERICAL EXAMPLES

In this section, we give some results of electromagnetic scattering obtained for the perfectly conducting plates.

Example one: Consider the bistatic radar cross section of a circular plate of diameter 3.18λ at normal incidence. Mesh sizes of $T = 0.061\lambda$ were used on the plate, giving 2145 nodes. The triangular basis is chosen for the expansion and weighting functions. The bistatic RCS curves for the E- and H-plane variations via the scattering angle are plotted in Figure 8.

Comparing with the analytical results in [21], we find that our results are very good.

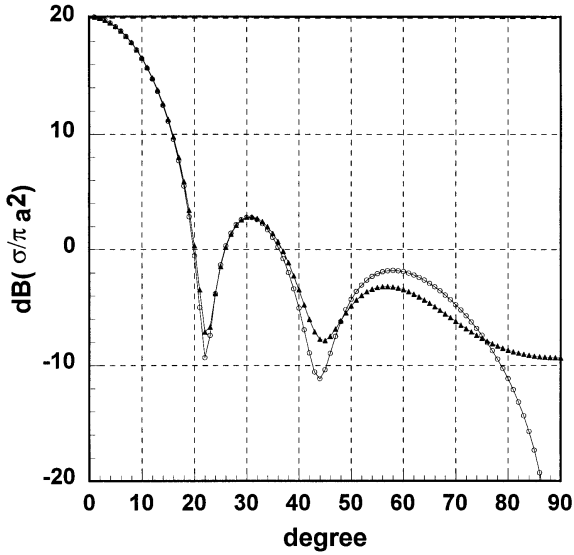

Figure 8. Bistatic scattering cross section on normal incidence ($\circ$: H-plane ; $\triangle$: E-plane) .

Example two: Consider the scattering from a $2\lambda \times 2\lambda$ perfectly conducting plate. The plate is discretized into 33×33 cells. The

mesh size is $T = 0.061\lambda$. The roof-top basis functions are chosen for the expansion and weighting functions. The number of unknowns $\{J_x, J_y\}$ are 1089 and 1024 respectively. The total unknowns of the linear equation is 2113.

The monostatic RCS of the plate versus the angle of incidence with E-polarized and H-polarized plane wave on the xoz plane are plotted in Fig. 9.

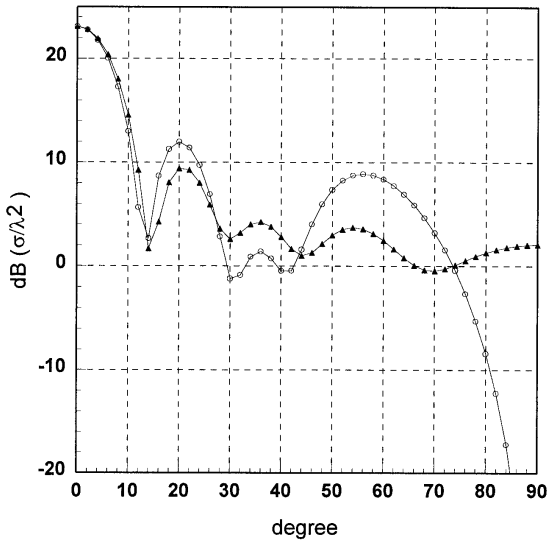

Figure 9. Monostatic scattering cross section on the xoz plane ($\circ$: H-polarization ; $\triangle$: E-polarization) .

Example three: Consider the scattering from an equilateral triangular perfectly conducting plate (2λ per side). The mesh size is $T = 0.061\lambda$. The roof-top basis functions are chosen for the expansion and weighting functions. The number of unknowns $\{J_x, J_y\}$ are 477 and 458 respectively. Total number of unknowns $\{J_x, J_y\}$ for the linear equation is 935.

The monostatic RCS of the plate versus the angle of incidence with E-polarized and H-polarized plane wave on the xoz plane are plotted in Fig. 10. Comparing the measured data and results of other researchers in [17, 18, 22], we find that our results are excellent.

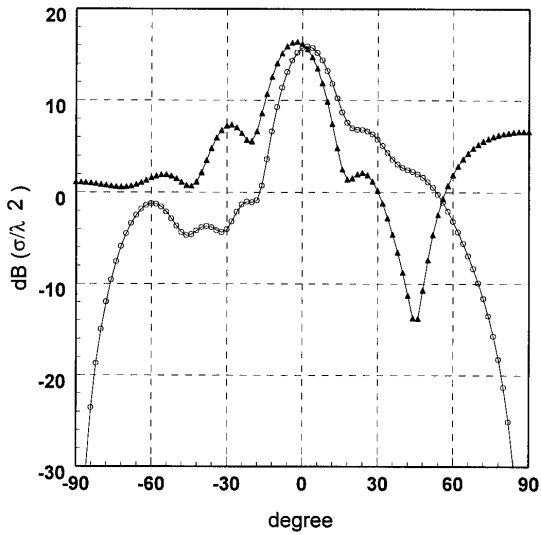

Figure 10. Monostatic scattering cross section on the xoz plane ($\circ$: H-polarization ; $\triangle$: E-polarization) .

4. CONCLUSION

The purpose of this paper was to present the new formula for computing the impedance matrix in the moment method. For the two kind of common basis functions, such as roof-top function and the product of the two triangular functions, the formula used to compute the elements of the impedance matrix were presented. Because the formula for a Galerkin's method in two dimension is a double integral, not a quadruple integral, it can save much more CPU time. The singularity of the integral can easily be removed through a suitable variable transform. Hence, the new method is more efficient and also quite accurate. By use of these new formulas, numerical examples of scattering problems of the conducting plates have been studied.

REFERENCES

1. Harrington, R. F., *Field Computation by Moment Method,* Hacmillan Press, New York, 1968.
2. Miller, E. K., L. Medgyesi-Mitschang, and E. H. Newman, Eds., *Computational Electromagnetics: Frequency-Domain Method of Moments,* New York: IEEE Press, 1992.
3. Steinberg, B. Z., and Y. Leviatan, "On the use of wavelet expansions in method of moments," *IEEE Trans. Antennas Propagat.,* Vol. AP–41, No. 5, 610–619, May 1993.
4. Goswami, J. C., A. K. Chan, and C. K. Chui, "On solving first-kind integral equations using wavelets on a bounded interval," *IEEE Trans. Antenna Propagat.,* Vol. AP–43, No. 6, 614–622, June 1995.
5. Wang, G., "A hybrid wavelet expansion and boundary element analysis of electromagnetic scattering from conducting objects," *IEEE Trans. Antennas Propagat.,* Vol. AP–43, No. 2, 170–178, February 1995.
6. Canning, F. X., "The impedance matrix localization method (IML) uses," *IEEE Trans. Antennas Propagat.,* Vol. AP-41, No. 5, 659–667, 1993.
7. Canning, F. X., "The impedance matrix localization method (IML) for MM calculation," *IEEE AP Magazine,* Vol. 32, 18–30, October 1990.
8. Coifman, R., V. Rohklin, and S. Wandzura, "The fast multipole method for the wave eqaution: A pedestrian prescription," *IEEE Antennas Propagat. Mag.,* Vol. 35, 7–12, 1993.
9. Rohklin, V., "Rapid solution of integral equations of scattering in two dimensions," *J. Comput. Phys.,* Vol. 86, 414–439, 1990.
10. Michielssen, E., and A. Boag, "Multilevel evaluation of electromagnetic fields for the rapid solution of scattering problems," *Microwave Opt. Tech. Lett.,* Vol. 7, No. 17, 790–795, December 1994.
11. Michielssen, E., and A. Boag, "A multilevel matrix decomposition algorithm for analyzing scattering from large structures," *11th Annu. Rev. Progress ACES,* Monterey, CA, 614–620, March 1995.
12. Michielssen, E., and A. Boag, "A multilevel matrix decomposition algorithm for analyzing scattering from large structures," *IEEE Trans. Antennas Propagat.,* Vol. AP–44, No. 8, 1086–1093, August 1996.
13. Su, C., and T. K. Sarkar, "A multiscale moment method for solving Fredholm integral equation of the first kind," *J. Electromag. Waves Appl.,* Vol. 12, 97–101, 1998.

14. Su, C., and T. K. Sarkar, "Electromagnetic scattering from coated strips utilizing the adaptive multiscale moment method," *Progress In Electromagnetics Research, PIER 18,* 173–208, 1998.
15. Su, C., and T. K. Sarkar, "Electromagnetic scattering from two-dimensional electrically large perfectly conducting objects with small cavities and humps by use of adaptive multiscale moment methods (AMMM)," *J. Electromag. Waves Appl.,* Vol. 12, 885–906, 1998.
16. Sarkar, T. K., *Application of Conjugate Gradient Method to Electromagnetics and Signal Analysis,* Elsevier Press, N.Y., 1991.
17. Peters, T. J., and J. L. Volakis, "Application of a conjugate gradient FFT method to scattering from thin planar material plates," *IEEE Trans. Antennas Propagat.,* Vol. 36, No. 4, 518–526, April 1988.
18. Barkeshli, K., and J. L. Volakis, "On the implementation of the conjugate gradient Fourier transform method for scattering by planar plates," *IEEE Trans. Antennas Propagat. Mag.,* Vol. 32, 19–29, April 1990.
19. Catedra, M. F., J. G. Cuevas and L Nuno, "A scheme to analyze conducting plates of resonant size using the conjugate gradient method and the fast Fourier transform," *IEEE Trans. Antennas Propagat.,* Vol. AP–36, No. 12, 1744–1752, December 1988.
20. Bleszynski, E., M. Bleszynski, and T. Jaroszewicz, "AIM: Adaptive integral method for solving large-scale electromagnetic scattering and radiation problems," *Radio Science,* Vol. 31, No. 5, 1225–1251, 1996.
21. Hodge, D. B., "Scattering by circular metallic," *IEEE Trans. Antennas Propagat.,* Vol. AP–28, No. 9, 707-712, September 1980.
22. Deshpande, M. D., C. R. Cockrell, F. B. Beck, E. Vedeler, and M. B. Koch, "Analysis of electromagnetic scattering from irregularly shaped, thin, metallic flat plates," *NASA Technical Paper,* NAS 1.60:3364, 1993.